



DS86760016, a Leucyl-tRNA Synthetase Inhibitor, Is Active against *Mycobacterium abscessus*

Thanh Quang Nguyen,^a Bo Eun Heo,^a Bui Thi Bich Hanh,^b Seunghyeon Jeon,^a Yujin Park,^a Arunima Choudhary,^a Sujin Lee,^{c,d} Tae Ho Kim,^b Cheol Moon,^e Sun-Joon Min,^{c,d,f}  Jichan Jang^{a,b}

^aDivision of Life Science, Department of Bio & Medical Big Data (BK21 Four Program), Research Institute of Life Science, Gyeongsang National University, Jinju, Republic of Korea

^bDivision of Applied Life Science (BK21 Four Program), Research Institute of Life Science, Gyeongsang National University, Jinju, Republic of Korea

^cDepartment of Applied Chemistry, Hanyang University, Ansan, Gyeonggi-do, Republic of Korea

^dCenter for Bionano Intelligence Education and Research, Hanyang University, Ansan, Gyeonggi-do, Republic of Korea

^eDepartment of Clinical Laboratory Science, Semyung University, Jecheon, Republic of Korea

^fDepartment of Chemical and Molecular Engineering, Hanyang University, Ansan, Gyeonggi-do, Republic of Korea

Thanh Quang Nguyen and Bo Eun Heo contributed equally to this work. Author order was determined in order of increasing seniority.

ABSTRACT Benzoxaboroles are a new class of leucyl-tRNA synthetase inhibitors. Epetraborole, a benzoxaborole, is a clinical candidate developed for Gram-negative infections and has been confirmed to exhibit favorable activity against a well known pulmonary pathogen, *Mycobacterium abscessus*. However, according to [ClinicalTrials.gov](https://clinicaltrials.gov), in 2017, a clinical phase II study on the use of epetraborole to treat complicated urinary tract and intra-abdominal infections was terminated due to the rapid emergence of drug resistance during treatment. Nevertheless, epetraborole is in clinical development for nontuberculous mycobacteria (NTM) disease especially for *Mycobacterium avium* complex-related pulmonary disease (MAC-PD). DS86760016, an epetraborole analog, was further demonstrated to have an improved pharmacokinetic profile, lower plasma clearance, longer plasma half-life, and higher renal excretion than epetraborole in animal models. In this study, DS86760016 was found to be similarly active against *M. abscessus in vitro*, intracellularly, and in zebrafish infection models with a low mutation frequency. These results expand the diversity of druggable compounds as new benzoxaborole-based candidates for treating *M. abscessus* diseases.

KEYWORDS *Mycobacterium abscessus*, leucyl-tRNA, benzoxaboroles, epetraborole, DS86760016, mutation frequency, drug resistance

Mycobacterium abscessus (*Mab*) is an environmental *mycobacterium*, and *Mab* is one of the most difficult-to-treat bacterial respiratory pathogen due to its intrinsic and acquired resistance to current anti-tuberculous drugs and antibiotics (1). To date, no antibiotic class or regimen has been effective for long-term sputum smear conversion in pulmonary *Mab* infections (2). Therefore, new and more effective anti-*Mab* drugs are needed. *Mab* drug pipelines primarily focus on reforming or repurposing approved antibiotics, and no new Food and Drug Administration (FDA)-approved antibiotics are currently available to treat *Mab* pulmonary diseases (2). Therefore, the discovery of novel drugs against *Mab* has received significant scientific attention; however, the current efforts remain insufficient.

Aminoacyl-tRNA synthetases (AARSs) are an essential and universally distributed family of enzymes that catalyze the covalent attachment of amino acids to their cognate tRNAs during translation (3). Among them, the prokaryotic leucyl-tRNA synthetase (LeuRS) plays a crucial role in bacterial protein synthesis and has become a major target for antimicrobial development (4). For example, in a study on *Mycobacterium tuberculosis* (*Mtb*) LeuRS, boron-containing compounds designed as LeuRS inhibitors through an oxaborole tRNA-trapping

Copyright © 2023 American Society for Microbiology. All Rights Reserved.

Address correspondence to Sun-Joon Min, sjmin@hanyang.ac.kr, or Jichan Jang, jichanjang@gnu.ac.kr.

The authors declare no conflict of interest.

Received 23 November 2022

Returned for modification 9 December 2022

Accepted 27 April 2023

Published 22 May 2023

(OBORT) mechanism by guiding X-ray crystallography exhibited good biochemical activity and excellent whole-cell activity against *Mtb* (5). Furthermore, Ganapathy et al. reported that antituberculosis 4-halogen benzoxaborole EC/11770 retained potency against drug-tolerant biofilms *in vitro* and *in vivo* in a mouse infection model (6). Recently, nonhalogenated benzoxaborole, epetraborole (ETB) (also known as GSK2251052 and AN3365), a clinically advanced lead candidate developed for Gram-negative bacterial infections, was narrowed down by an *in vitro* dual screen against *Mab* using a pandemic response box chemical compound library; it exhibited effective *in vivo* efficacy in a *Mab*-infected zebrafish (ZF) model (7). ETB was further studied in a mouse infection model by Ganapathy et al., and it (300 mg/kg) exhibited similar *in vivo* efficacy to that of clarithromycin treatment (250 mg/kg) (6). Thus, ETB may be a new candidate drug for treating *Mab* lung diseases.

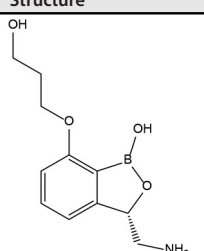
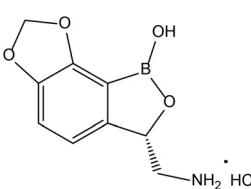
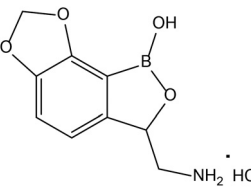
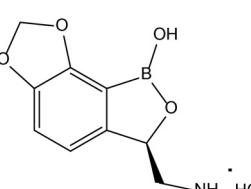
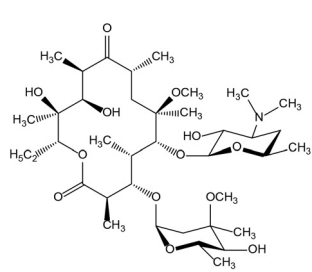
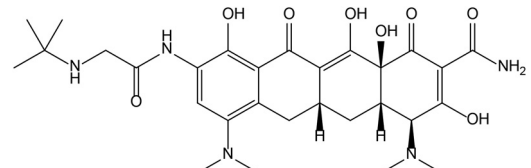
However, according to [ClinicalTrials.gov](https://clinicaltrials.gov), in 2017, a clinical phase II study on the use of ETB to treat complicated urinary tract and intra-abdominal infection was discontinued due to the rapid emergence of drug resistance during treatment (8). Nevertheless, ETB is currently in clinical development for nontuberculous mycobacteria (NTM) disease especially for *Mycobacterium avium* complex-related pulmonary disease (MAC-PD) by AN2 Therapeutics. Furthermore, ETB was granted orphan medicinal product designation in NTM lung disease in the European Union (9). Recently, a novel LeuRS inhibitor, DS86760016 (DS), potent against a multidrug-resistant (MDR) *Pseudomonas aeruginosa*, has been developed. DS showed an improved pharmacokinetic profile, lower plasma clearance, longer plasma half-life, and higher renal excretion than ETB in an animal model (10). Additionally, DS had a lower frequency of drug resistance than ETB in comparative *in vivo* studies using murine urinary tract infection models (11). In this study, we synthesized DS, and its activity was tested against *Mab in vitro*, intracellularly, and in ZF and compared with that of ETB. Furthermore, the spontaneous resistance frequencies of *Mab* against ETB and DS were compared. The results suggest that DS is a potentially new candidate drug for treating *Mab* lung infections, with lower drug spontaneous resistance frequency than ETB.

RESULTS

***Mab* susceptibility to benzoxaboroles.** To compare the *in vitro* activity of ETB and DS against *Mab*, an ETB analog was synthesized as racemic mixture and separated enantiomers (Fig. S1) (12), and their activity was tested against two types of *Mab*: *Mab* Collection de l'Institut Pasteur (CIP) 104536^T smooth (S) and rough (R) morphotypes. Resazurin-based drug-susceptibility tests in a cation-adjusted Mueller-Hinton (CAMH) medium were performed with reference compounds such as clarithromycin (CLA) and tigecycline (TGC). During the course of the synthesis of DS as an optically active form, we initially synthesized racemic (\pm)-DS to optimize the entire synthetic processes for DS. Next, the first chiral intermediate (compound **5** in Fig. S1) was separated through a chiral high-performance liquid chromatography (HPLC) chromatographic method to afford optically active (*S*)-**5** and (*R*)-**5**, respectively (13). Each enantiomer **5** was subject to reduction followed by salt formation to give DS or ($-$)-DS as an optically pure compound. Thus, the inhibitory activities of all the synthesized DS compounds (both optically active DS enantiomers, and racemic [\pm]-DS) against *Mab* were evaluated (Table 1). MIC₅₀ was defined as the minimum concentration required to inhibit 50% growth of the organism, and the MIC₅₀ value of ETB for *Mab* (S) CIP104536^T growth was 0.3 μ M. Moreover, DS exerted strong inhibitory activity, with an MIC₅₀ as low as 0.7 μ M for the *Mab* (S) CIP104536^T and 0.9 μ M for the *Mab* (R) CIP104536^T morphotype, comparable to ETB (Fig. 1A; Table 1). In addition, (\pm)-DS showed significant *in vitro* activity. In contrast, ($-$)-DS showed very high MIC₅₀ values ($>20 \mu$ M). CLA and TGC were used as positive controls, which also effectively inhibited *Mab* growth (Table 1).

To investigate the potential activity of the *S* enantiomer/(+)-DS86760016, the activity of DS against three type strains (*Mab* subsp. *abscessus* CIP104536^T, *Mab* subsp. *massiliense* CIP108297^T, and *Mab* subsp. *bolletii* CIP108541^T), 10 clinical isolates of *Mab*, and 10 type strains of different nontuberculous mycobacterial (NTM) species was determined. Foremost, all the subspecies tested were susceptible to DS (Fig. 1B). The range of MIC₅₀ values of DS

TABLE 1 Chemical structures and MIC₅₀ values of benzoxaboroles, clarithromycin, and tigecycline against *M. abscessus* smooth and rough morphotype

Compound	Structure	MIC ₅₀ (μM)	
		<i>M. abscessus</i> smooth	<i>M. abscessus</i> rough
Epetraborole (ETB)		0.3	0.3
DS86760016 (DS)	 (+)-DS86760016	0.7	0.9
(±)-DS86760016	 (±)-DS86760016	1.5	2.0
(-)-DS86760016	 (-)-DS86760016	22.0	23.5
Clarithromycin (CLR)		4.9	5.6
Tigecycline (TGC)		0.7	0.9

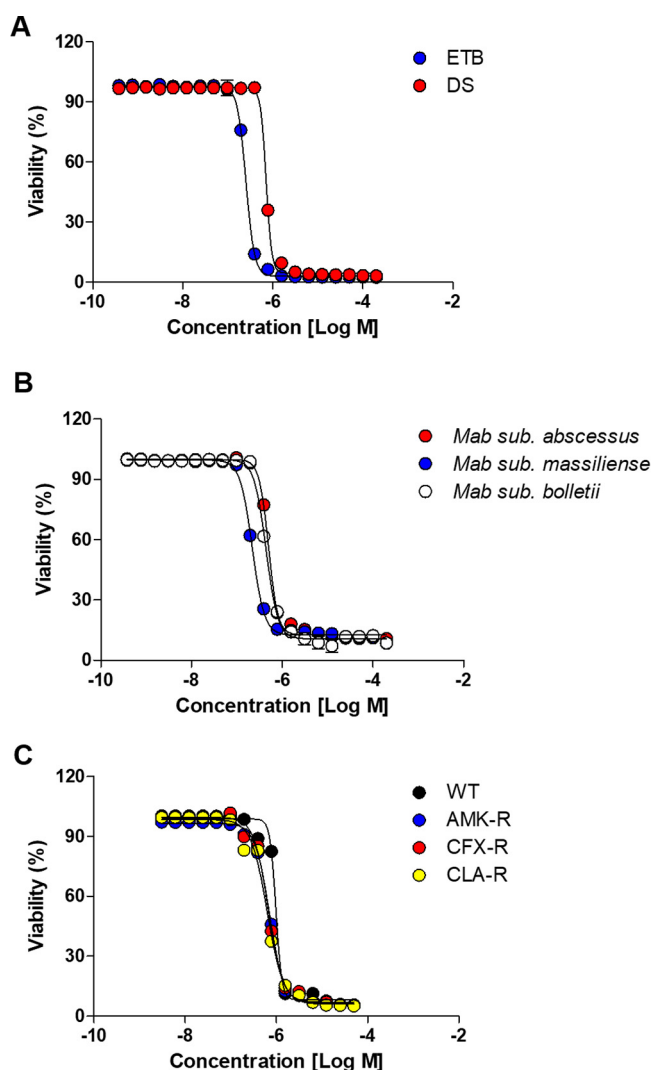


FIG 1 Susceptibility test against *Mab* strains. (A) Activity of epetaborole (ETB) and DS86760016 (DS) against *Mab* CIP104536^T (S) morphotype. (B) *In vitro* activity of DS was evaluated against *Mab* subspecies such as *Mab* subsp. *abscessus* CIP104536^T, *Mab* subsp. *massiliense* CIP108297^T, and *Mab* subsp. *bolletii* CIP108541^T by the resazurin microtiter assay (REMA). (C) DS activity against AMK-resistant (AMK-R), CFX-resistant (CFX-R), and CLA-resistant (CLA-R) strains. Dose-response curves were plotted using the GraphPad Prism software (version 6.05). The data are expressed as the means \pm standard deviation (SD) of triplicates for each concentration. WT, wild type.

for the strains was 0.2 to 0.5 μ M. Next, the possible inhibitory effect of DS on the growth of drug-resistant strains generated *in vitro* at high concentrations of amikacin (AMK), ceftazidime (CFX), and CLA (14) was analyzed. The laboratory-generated AMK-, CFX-, and CLA-resistant mutants (AMK-R, CFX-R, and CLA-R) were fully inhibited by DS, with the same MIC range as that of the wild types (WTs) (Fig. 1C). Furthermore, DS activity against the clinical isolates of *Mab* with smooth (S) and R morphotypes was evaluated. Both ETB and DS were effective against 10 *Mab* clinical isolates that were selected from the Korean Mycobacterial Resource Center (KMRC) (Table 2). Significant growth inhibition was observed when the clinical isolates of *Mab* were treated with various concentrations of ETB and DS. MIC₅₀ values ranged from 0.4 to 3.3 μ M for ETB and 0.7 to 6.5 μ M for DS. TGC was used as a positive control, which effectively inhibited the growth of *Mab* strains. Given the activity of DS against *Mab* (Table 1 and 2), its possible activity against other NTM members was evaluated. DS was tested against 10 different NTM species and was found to be active against other NTMs, including *Mycobacterium avium* strains, the most common causative agent of NTM lung disease (Table 3). Thus, DS has broad-spectrum antimycobacterial activity, similar to that of ETB.

TABLE 2 MIC₅₀ values of the compounds against 10 clinical *M. abscessus* isolates^a

Korean Mycobacterial Resource Center Strains	Morphotype	<i>erm</i> (41) sequevar	MIC ₅₀ (μM)		
			ETB	DS	TGC
00136-61038	S	T28	1.5	3.1	0.7
00136-61039	S	C28	0.4	0.7	0.7
00136-61040	R	T28	3.2	6.5	0.8
00136-61041	S	T28	0.9	1.8	0.7
00200-61198	S	C28	0.7	1.5	0.7
00200-61199	S	T28	1.8	3.8	0.7
00200-61200	S	T28	0.7	2.7	0.7
00200-61201	S	T28	0.7	1.5	0.7
00200-61202	R	T28	3.3	6.2	0.8
00200-61204	S	T28	1.6	3.7	0.7

^aT28 sequevars provide inducible clarithromycin resistance. C28 sequevars are clarithromycin sensitive. *erm*(41), erythromycin ribosome methyltransferase; DS, DS86760016; ETB, epetaborole; R, rough; S, smooth; TGC, tigecycline.

DS activity against intracellular replicating *Mab*. The potency of DS against *Mab* replication in the host cells was investigated. Green fluorescence expressing *Mab* (S) CIP104536^T-mWasabi was used to infect mouse bone marrow-derived macrophages (mBMDMs), and the growth inhibitory effect of DS was observed using a cell-based phenotypic assay with an automated cell imaging system. Dimethyl sulfoxide (DMSO) (untreated control) was used as the negative control. After DS was dose-dependently added to the *Mab* (S) CIP104536^T-mWasabi-infected mBMDMs cells, images were captured and analyzed. To quantify different parameters, such as the number of host macrophages, the percentage of infected cells, and the total fluorescence intensity, CellReporterXpress image acquisition and analysis software was used. The yellow colors indicate the merging of *Mab* (S) CIP104536^T-mWasabi engulfed by red-stained macrophages through phagocytosis. As shown in Fig. 2A, significant intracellular *Mab* (S) CIP104536^T-mWasabi green fluorescent signal were observed in DMSO-treated cells. However, DS had a significant intracellular activity similar to that of ETB treatment at 0.1 μM. In more details, the percentage of intracellular *Mab* (S) CIP104536^T-mWasabi at different concentrations of ETB and DS were compared. ETB-treated (Fig. 2B) and DS-treated (Fig. 2C) mBMDMs showed a significantly reduced mWasabi fluorescent pixel intensity in a compound dose-dependent manner (blue dots). Furthermore, there was no cell number reduction by ETB and DS treatment at any tested concentration (red dots). These results demonstrate that ETB and DS can penetrate the host cell membrane and inhibit intracellular *Mab*. This fluorescent-based intracellular activity was further validated. The number of live *Mab* (S) inside mBMDMs was determined by the traditional colony count method after lysis of the infected cells treated with DS and ETB, respectively. As shown in Fig. 2D, DS significantly decreased the number of intracellular mycobacteria after infection at concentrations of 1 μM. DS treatment led to a 4.4 log₁₀ reduction in mycobacteria, which was comparable to that elicited by ETB (3.3 log₁₀ reduction). CLA 0.1 × MIC was used as control. Hence, we concluded that DS was active against intracellular *Mab* (S).

TABLE 3 Broad-spectrum activity of compounds for other mycobacteria

Species	MIC ₅₀ (μM)		
	ETB	DS	TGC
<i>M. smegmatis</i>	0.2	0.3	0.9
<i>M. chelonae</i>	1.3	2.4	3.8
<i>M. fortuitum</i>	0.2	0.3	2.3
<i>M. vaccae</i>	0.3	0.4	1.9
<i>M. goodii</i>	0.7	1.5	3.0
<i>M. terrae</i>	0.8	2.8	5.1
<i>M. avium</i>	0.2	0.4	5.8
<i>M. marinum</i>	1.3	2.6	2.8
<i>M. szulgai</i>	0.6	0.9	1.2
<i>M. intracellulare</i>	0.2	0.3	5.6

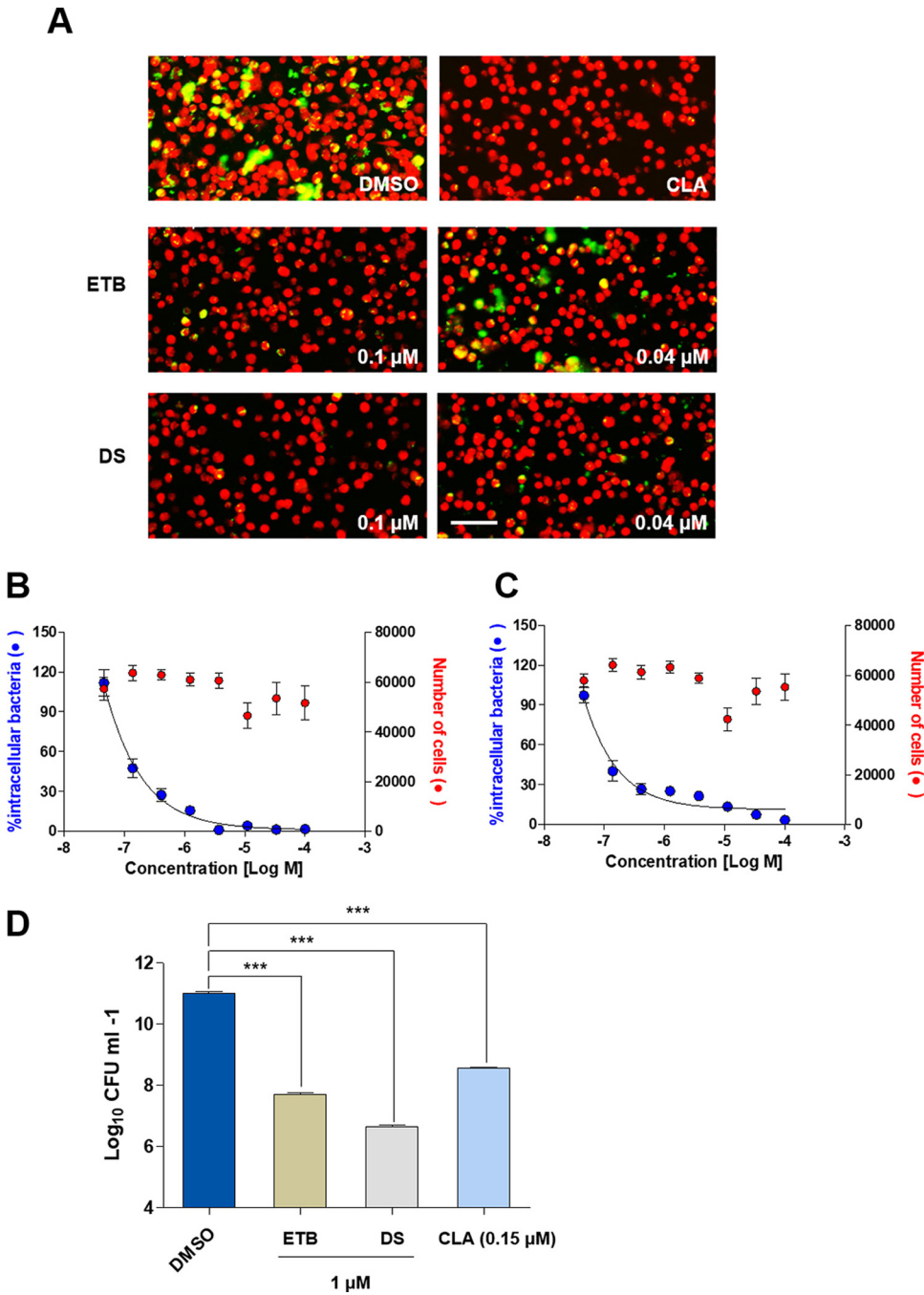


FIG 2 Intracellular activity of ETB and DS against *Mab(S)*-*mWasabi*. Images of *Mab(S)*-*mWasabi*-infected mBMDMs on day 3 after treatment with different doses of ETB and DS. Dimethyl sulfoxide (DMSO) was used as negative control. Mouse bone marrow-derived macrophages (mBMDMs) were stained with syto60 (red), and the cells were analyzed using the automated cell imaging system. (A) The yellow colors represent *Mab(S)*-*mWasabi* that were phagocytized by red-stained mBMDM cells. Bar, 52.44 μm . (B, C) Pixel intensities of *Mab(S)*-*mWasabi* in mBMDMs (blue dot) and total number of cells (red dot) were quantified after treatment of cells with different concentrations of ETB (B) and DS (C). (D) For the traditional CFU quantification, mBMDMs were infected at a multiplicity of infection (MOI) of 3 with *Mab(S)* and treated with ETB, DS, and CLA. The experiment was performed in triplicate, and the results are shown as the means \pm standard deviation (SD). ***, $P < 0.001$.

DS exerts anti-*Mab* activity in Zebrafish. To determine the therapeutic potential of DS, the *in vivo* efficacy of DS was evaluated in ZF after infection with the *Mab* (R) CIP104536^T, which is hypervirulent in the C57/BL6 mice model (15). ZF was infected with *Mab* (R) CIP104536^T, and the efficacy of DS was compared to that of ETB at concentrations of 6.25, 12.5, 25, and 50 μM . The *in vivo* efficacy was evaluated in two different approaches.

First, the number of live *Mab* (R) CIP104536^T in ZF after DS or ETB was enumerated by quantifying CFU per ZF. After 5 days of treatment, a statistically significant bacterial load reduction was observed at each tested concentration (25 and 50 μM), demonstrating that DS and ETB killed *Mab* (R) CIP104536^T in ZF. DS treatment at 50 μM yielded approximately 3.9 \log_{10} CFU reduction on an agar plate compared to the untreated control, similar to ETB treatment at 50 μM . Furthermore, the effectiveness of DS and ETB at 50 μM was comparable to that of TGC (50 μM) (Fig. 3A).

Second, the potential for increased DS concentration to expand the life span of *Mab* (R) CIP104536^T-infected ZF in comparison with ETB was evaluated. The survival rate of ZF was monitored using the Kaplan-Meier method for 13 days postinfection (dpi) after treatment with each drug. All the ZF in the untreated group died at 13 dpi (Fig. 3B). However, the DS- and ETB-treated groups showed a concentration-dependent significantly increased ZF life span (Fig. 3C). ZF survival was 35% and 42% when *Mab* (R) CIP104536^T-infected ZF was exposed to 12.5 and 25 μM DS, respectively, but increased exponentially to 80% at 50 μM DS, similar TGC at 50 μM . ETB also showed a similar survival curve to that of DS at the same concentration (Fig. 3C). Taken together, these results demonstrate that DS exerts a therapeutic effect on *Mab* *in vivo*.

Resistance frequency comparison between DS and ETB. To compare the rates of *Mab* resistance to DS and ETB, DS- and ETB-resistant mutant frequencies at different concentrations were evaluated. The *Mab* (S) CIP104536^T culture was plated on Middlebrook 7H10-OADC containing DS and ETB, respectively (1 \times , 2 \times , 4 \times , and 8 \times MIC). After 5 days of incubation, the colonies that appeared were considered resistant (moderate-level resistance). The mutation frequencies of the *Mab* ETB-resistant isolates ranged from 3.4×10^{-7} to 4.2×10^{-8} , and the mutation rate of the *Mab* DS-resistant isolates ranged from 8.0×10^{-8} to 8.0×10^{-9} (Table 4). The mutation frequency of DS was 4.5 times (median) lower than the range determined for ETB. From the resistant mutants, five mutants that showed the strongest resistance to DS were isolated. Furthermore, we also generated two more DS high-level resistant strains at 100 μM DS. Using both moderate- and high-level resistant strains, we evaluated their resistance against DS compared with that of the WT. As shown in Fig. 4A and Table 5, all of the DS-resistant strains tested showed very high MIC values against DS in comparison with WT. Moreover, both of these DS-R high strains showed resistance not only to DS but also to ETB (Table S1). However, all laboratory-generated DS-resistant mutants were fully inhibited by TGC. All the DS-resistant mutants tested were as sensitive to TGC as the WT, with the similar MIC range and without differences between the strains (Fig. 4B). Therefore, the DS-resistant mutants were genuine DS-specific mutants. To validate the molecular targets of DS, *leuS* (MAB_4923c), which encodes LeuRS and is a molecular target of ETB, DS-resistant mutants were sequenced. Sequencing results showed that four of five had missense mutations in various amino acids in LeuS (Table 5). Nine different amino acid sites in LeuS were observed as missense mutations in six different DS-resistant mutants (D284G, Q345R, Y420C, I426T, R435C/L/S, D436A, V468L, N469Y, and E524K). These results suggest that DS targets LeuS to exert its anti-*Mab* activity as an ETB.

DISCUSSION

AARSs are essential enzymes that ligate amino acids to tRNAs and translate their genetic code during protein synthesis. Thus, the development of small molecule therapeutics against AARSs in infectious diseases has been spotlighted (16). So far, there are numerous LeuRS inhibitors that show anti-*Mab* activity. EC/11770 and GSK656, which were initially developed as anti-*Mtb* agents, also showed good *in vitro* activity against *Mab*. Additionally, EC/11770 reduced the bacterial burden at 10 mg/kg in a *Mab* subsp. *abscessus* K21 strain (clinical isolate)-infected NOD.CB17-Prkdcscid/NCrCrI (NOD SCID) model of lung infection (6). Recently, novel boron-containing LeuRS inhibitor MRX-6038 was developed by Shanghai MicuRx Pharmaceutical Co., Ltd., and this compound showed high anti-*Mab* activity against extracellular *Mab* subsp. *massiliense* CIP108297 in culture, with a MIC₅₀ of 0.063 mg/liter and a MIC₉₀ of 0.125 mg/liter (17). Moreover, MRX-6038 showed a significant reduction in the bacterial load in the lungs of *Mab*-infected neutropenic induced mice model (7.8 \log_{10} CFU/

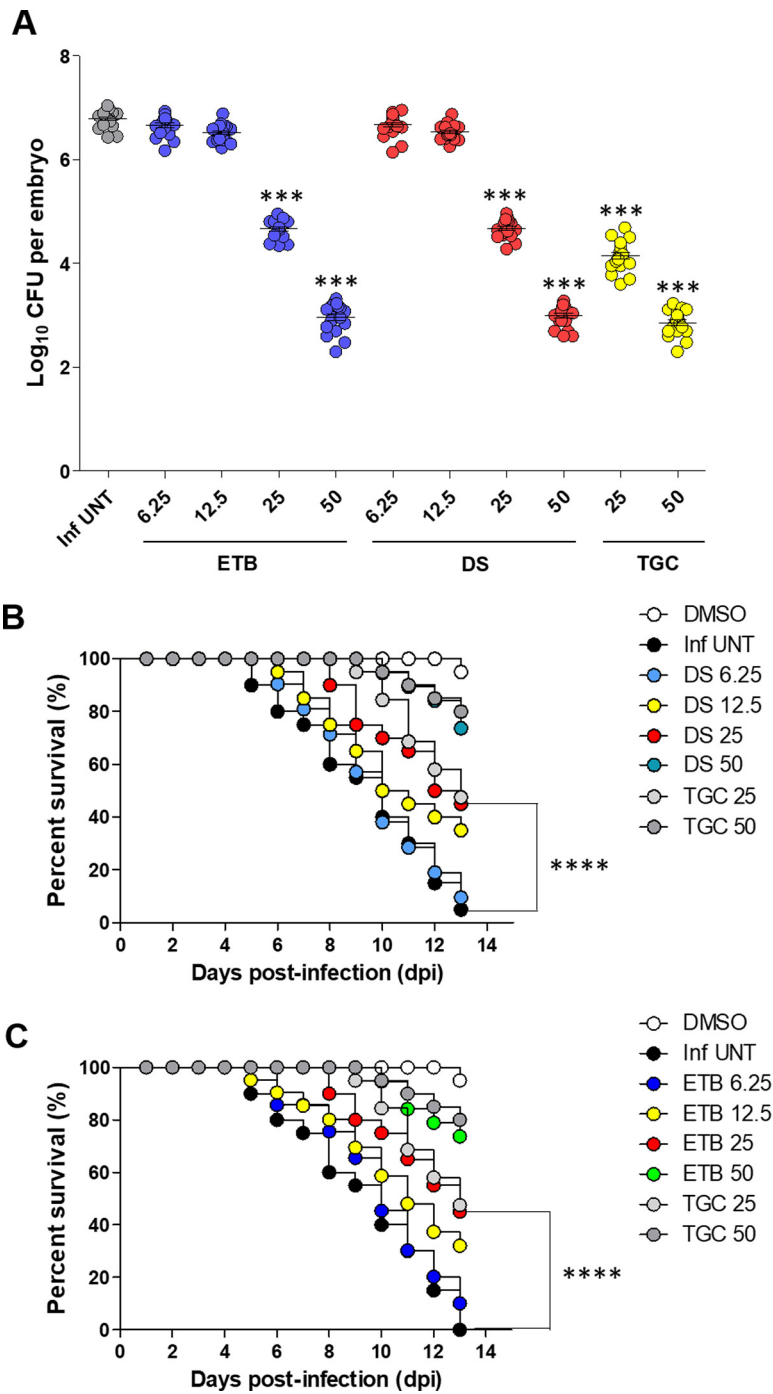


FIG 3 Evaluation of *in vivo* compound activity on *Mab* (R) CIP104536^T. The *Mab* (R) CIP104536^T burden of untreated or ETB- and DS-treated embryos is shown. The results are expressed as mean log₁₀ CFU per embryo from three independent experiments. (A) Significant difference compared with untreated control. ****, *P* < 0.0001. (B, C) Survival of *Mab* (R) CIP104536^T-infected embryos treated at 6.25, 12.5, 25, and 50 μM DS (B) and ETB (C) in comparison with untreated infected embryos (*n* = 20, representative of three independent experiments). Survival curves were compared with log-rank (Mantel-Cox) test. ****, *P* < 0.0001. dpi, days postinfection; Inf UNT, infected untreated; TGC, tigecycline.

lung reduction) compared to the untreated group (17). Previously, our group identified ETB against *Mab* by screening a Medicines for Malaria Venture (MMV) pandemic response box containing 400 diverse drug-like molecules active against bacteria, viruses, or fungi and established its efficacy against *Mab* in a ZF infection model (7). ETB exhibited favorable *in vitro* activity against *Mab* subsp. *abscessus* CIP104536 (rough morphotype) with MIC

TABLE 4 Mutation frequency of *M. abscessus* in different concentration of ETB and DS

Compound	1 × MIC	2 × MIC	4 × MIC	8 × MIC
ETB	3.4×10^{-7}	1.5×10^{-7}	1.3×10^{-7}	4.2×10^{-8}
DS	8.0×10^{-8}	3.3×10^{-8}	2.9×10^{-8}	8.0×10^{-9}
Fold change	4.3	4.5	4.5	5.3

range from 0.014 to 0.046 mg/liter and it displayed 1 log₁₀ bacterial burden reduction in mice model that administered a 300 mg/kg dose orally (18, 19). However, in a phase II clinical study on the use of ETB to treat patients with complicated urinary tract infections, the rapid emergence of drug resistance was observed, which prompted GlaxoSmithKline (GSK) to terminate the ETB development program. Nevertheless, a new oxaborole, DS, has reignited interest in LeuRS inhibitors, with a lower resistance than ETB, in comparative murine urinary tract infection models (10). However, DS is not commercially available because the pharmaceutical company (Daiichi Sankyo India) responsible for its discovery was shut down in 2017 (N. Masuda, personal communication). For this reason, we synthesized DS in-house and evaluated its activity against *Mab* *in vitro*, intracellularly, and in zebrafish models.

Here, we evaluated the activity of DS in different ways. First, the *in vitro* susceptibility of *Mab* cells to DS was tested. DS showed significantly lower growth inhibitory activity (submicromolar) against *Mab*, although its MIC was slightly higher than that of ETB. Among the racemic (±)-DS and optically active DS enantiomers, we confirmed that the most potent compound is DS possessing (S)-absolute configuration, of which the stereochemistry is identical to that of ETB. This result indicated that the spatial disposition of aminomethyl substituent in both DS and ETB plays an important role in inhibitory activity of three substituted benzoxaboroles against LeuRS in *Mab*. Moreover, DS exerted activities against the *Mab* S and R morphotypes, with similar MIC values (0.7 and 0.9 μM, respectively). The R morphotype could emerge from cystic fibrosis (CF) patients chronically colonized with an S strain and is more virulent, inducing a more aggressive, invasive pulmonary infection. In addition, the R morphotype is more proinflammatory than the S morphotype (20). Intravenous (IV) *Mab* infection

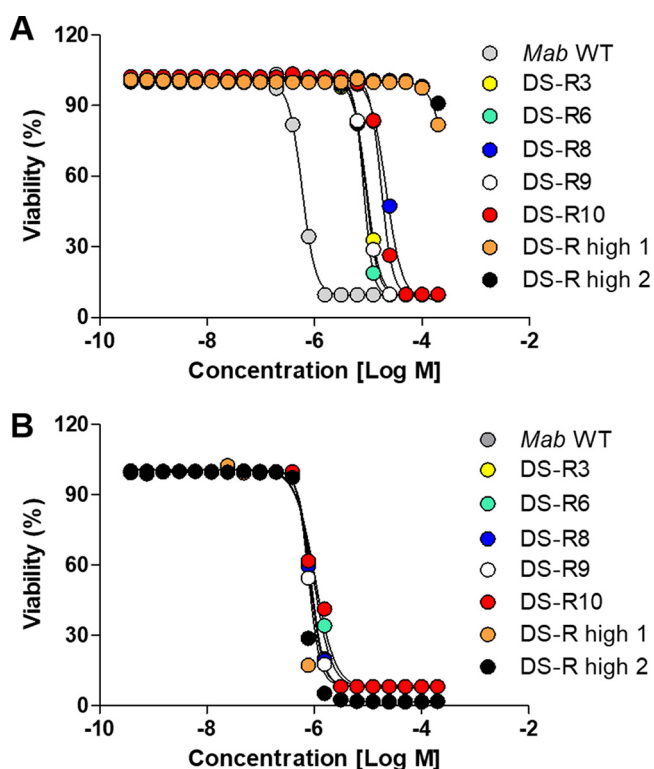
**FIG 4** Validation of DS-specific resistant mutant. Laboratory induced DS-resistant strains were tested for *in vitro* susceptibility for DS (A) and TGC (B), respectively. *Mab*, *Mycobacterium abscessus*.

TABLE 5 MICs and mutations in *LeuS* gene of DS-resistant strains^a

Strains	MIC ₅₀ (μM)		LeuS mutation
	DS	TGC	
<i>M. abscessus</i> wild type	0.6	0.9	ND
DS-R3	9.3	1.0	ND
DS-R6	8.2	1.0	<u>R435C</u> , <u>D436A</u> , N469Y
DS-R8	21.5	0.8	D284G, Q345R, <u>R435L</u> , V468L
DS-R9	8.9	0.8	D284G, Q345R, <u>R435L</u>
DS-R10	17.4	1.0	I426T, <u>R435S</u>
DS-R high 1 (generated at 100 μM)	>500	0.6	Y420C, <u>R435S</u> , E524K
DS-R high 2 (generated at 100 μM)	>290	0.7	I426T, <u>R435S</u> , E524K

^aUnderlining indicates previously reported mutations. ND, not determined.

mice models showed more lethal and higher levels of induced tumor necrosis factor- α (TNF- α) with the R morphotype than with the S morphotype (21–24). Thus, the effectiveness of the DS on the R morphotype would provide a better understanding of CF treatment. This *in vitro* activity was expanded further for *Mab* subspecies, laboratory-generated drug-resistant (AMK-, CFX-, and CLA-resistant) strains, and clinical isolates. The survival of all *Mab* strains significantly dose-dependently decreased in the presence of DS (Fig. 1; Table 2). In addition, DS showed favorable potency against NTMs. The low MIC value of DS for NTM indicates that DS is a broadly active antimycobacterial agent (Table 3). Furthermore, DS inhibited the growth of intracellular *Mab* without cytotoxicity, and it showed excellent *in vivo* efficacy in the ZF infection-treatment model. Nevertheless, DS activity against infection in higher animal models is yet to be determined. Testing the efficacy of DS in immunocompromised mice, such as NOD.CB17-*Prkdc*^{scid}/Ncr mice, will provide a better understanding of DS activity against *Mab* in the foremost mammalian model (6, 18, 19, 25, 26).

Finally, the frequency of DS resistance mutants was evaluated. The weakest point of ETB was the rapid emergence of resistance to the complicated urinary tract and intra-abdominal infections. In this study, a comparison of spontaneous resistance frequencies for DS and ETB was conducted, and DS showed an approximately 4.7 times lower mutation frequency than ETB for every drug concentration tested (Table 4). Furthermore, we identified several *leuS* mutation sites, not only amino acid positions 435 and 436, which were previously reported (underlined in Table 5), but also new mutation sites from DS-resistant mutants (18). Interestingly, the DS-R3 mutation did not exhibit any mutations in the *leuS* protein. To verify this novel DS resistance, we performed whole-genome sequencing (WGS) experiments with DS-R3, which does not contain the *leuS* mutation, as well as on the DMSO (control) and DS-R strains (with *leuS* mutation). From the WGS, we identified DS-R3 specific missense mutations in the MAB_0346 and MAB_2176 genes rather than the *leuS* gene (data not shown). According to information available on Mycobrowser (<https://mycobrowser.epfl.ch/>), MAB_0346 encodes a hypothetical protein, while MAB_2176 encodes an ABC transporter permease protein. Further investigation of these two genes will be conducted in future studies. Taken altogether, *Mab* therapy requires a combination of multiple drugs; therefore, multidrug therapy with DS will reduce DS-resistant mutant generation.

In conclusion, this study demonstrates DS, an advanced new LeuRS inhibitor at the preclinical development stage for Gram-negative infections, has potent against *Mab* *in vitro*, intracellularly and in ZF infection models. The discovery of DS activity against *Mab* will expand the diversity of druggable compounds as a new LeuRS inhibitory candidate for treating *Mab* diseases.

MATERIALS AND METHODS

Bacterial strains and culture conditions. *Mab* subsp. *abscessus* CIP104536^T variant was kindly provided by Laurent Kremer (CNRS, IRIM, Université de Montpellier, Montpellier, France). *Mab* subsp. *bolletii* CIP108541^T and *Mab* subsp. *massiliense* CIP108297^T were obtained from the Collection de l'Institut Pasteur (CIP, Paris, France). Clinical isolates were purchased from the Korea *Mycobacterium* Resource Center (KMRC, Osong, South Korea). Laboratory-generated resistant mutants against amikacin, ceftiofloxacin, and clarithromycin were induced under the high concentration of antibiotics and confirmed by sequencing. *Mab* strains were routinely grown at 37°C in cation-adjusted Mueller-Hinton (CAMH) medium (Sigma, St. Louis, MO, USA)

supplemented with 20 mg/liter calcium chloride (Sigma, St. Louis, MO, USA) and 10 mg/liter magnesium chloride (Sigma, St. Louis, MO, USA). *Mab* CIP104536 R strain harboring pMV262-mWasabi expressing of green fluorescent protein (GFP) under the selection of kanamycin 50 mg/liter was grown at 37°C, with shaking at 100 rpm in Middlebrook 7H9 broth that contained 0.2% glycerol (vol/vol), 0.05% Tween 80 (vol/vol) and was supplemented with albumin-dextrose-catalase (ADC) (vol/vol) (7H9^{G^T/ADC}).

Synthesis of racemic and optically active DS. According to the procedures reported in the literature, racemic DS and its optically active compounds were synthesized starting from 2-bromo-3-hydroxy-4-methoxybenzaldehyde as described in Fig. S1. The detail experimental procedures and characterization data of the synthesized compounds are provided in the additional experimental details.

MICs determination using resazurin microtiter assay (REMA). The MIC values were determined by using the resazurin microtiter assay (REMA). Briefly, bacterial stocks from the exponential-phase cultures were eluted to an optical density at 600 nm (OD₆₀₀) of 0.01. Fifty μ L of bacterial culture were used per well, and 50 μ L of serial 2-fold dilutions of test compound solution was added to each well of a sterile, polystyrene 96-well cell culture plate (SPL, Gyeonggi-do, South Korea). Each plate also contained a drug-free growth control. To avoid evaporation during incubation, 200 μ L of sterile water was added to outer perimeter wells. The plates were then covered with self-adhesive membranes and incubated at 37°C for 5 days. Then, 40 μ L of the 0.025% (wt/vol) resazurin solution was added to each well before, and the plates were reincubated overnight. Fluorescence was measured using a SpectraMax M3 multimode microplate reader (Molecular Devices, Sunnyvale, CA, USA). The dose-response curve was constructed, and the concentrations required to inhibit bacterial growth by 50% (MIC₅₀) were determined by GraphPad Prism software (version 6.05; San Diego, CA, USA).

Resistant mutant frequency determination. A total of 250 μ L of *Mab* S morphotype culture from the exponential-phase cultures were spread on Middlebrook 7H10 (BD Biosciences, catalog no. 262710) containing 0.05% Tween 80 (vol/vol), 10% oleic acid-ADC (OADC) supplemented with 0, 1 \times , 2 \times , 4 \times , and 8 \times MIC₉₀ of ETB and DS. The plates were incubated for 5 days at 37°C, and the colonies were counted. The mutation frequency was calculated from the median number of mutants divided by the viable count. Laboratory-generated resistant mutants against DS were generated under the medium containing 4 \times and 8 \times MIC₉₀ (1.05 μ M) of DS and confirmed by sequence using the primers *Mab*LeuRS (*Mab*4923c;_954bp)-F, 5'-CATATCGCCTGGTGTACCAAT-3'; and *Mab*LeuRS(*Mab*4923c;_954bp)-R, 5'-CGACGGTAATACGTTCTCAC-3'. Whole-genome sequencing (WGS) of the DS-resistant mutants was performed on the Illumina NovaSeq6000 by DNA Link, Inc. (Seoul, South Korea). Base-calling was performed using bcl2fastq2 (version 2.20) software.

Isolation of BMDMs and intracellular bacterial replication assay. Bone marrow-derived macrophages (BMDMs) were collected by flushing femur and tibia of 6-week-old C57BL/6 (KOATECH, Gyeonggi-di, Pyeongtaek-si, South Korea). BMDMs were cultured in Dulbecco's modified Eagle's medium (DMEM; Welgene, Gyeongsang-si, Gyeongsangbuk-do, South Korea) containing 10% fetal bovine serum (FBS; Welgene), GlutaMax (35050-061; Gibco), and penicillin/streptomycin (15140-122; Gibco) at 37°C and 5% CO₂. For differentiation into mBMDM, cells were exposed to recombinant murine macrophage colony-stimulating factor (M-CSF; JW-M003-0025, JW CreaGene) for 5 days.

For test antibacterial activity of the DS against intracellular bacteria, the cells were infected for 3 h with mWasabi protein-expressing *Mab* CIP104536^T S morphotype (here, *Mab* [S] CIP104536^T-mWasabi) at a multiplicity of infection of 1 in 96-well plates. After infection, extracellular bacteria were killed by treatment of 250 μ g/mL amikacin for 2 h. We washed the cells with phosphate-buffered saline (PBS; Gibco) and then treated them with compounds serially diluted in 96-well plates.

Intracellular bacterial replication assay. For test antibacterial activity of the DS against intracellular bacteria, mBMDMs were infected with *Mab*(S)-mWasabi (*Mab* CIP104536 S expressing green fluorescent protein) at a multiplicity of infection (MOI) of 1 for 3 h in 96-well plates. After infection, extracellular bacteria were killed by treatment of 250 μ g/mL amikacin for 2 h. We washed the cells with PBS (Gibco) and then treated them with serially diluted compounds for 3 days. The cells were stained with SYTO60 red fluorescent nucleic acid stain Invitrogen for quantifying the number of host macrophage and infected macrophage. Fluorescent images were estimated and analyzed by ImageXpress Pico automated imaging system (Molecular Devices). Colony-forming unit assay was also performed for counting the bacterial loads in the cells. The cells were lysed with 1% SDS (151-21-3; Genaray Biotechnology) to release intracellular bacteria. The lysates were serially diluted 10-fold with PBS. Each bacterial dilution was plated on 7H10-OADC supplemented by 50 μ g/mL kanamycin and incubated for at least 3 days at 37°C. After 3 days of incubation, bacterial colonies were counted.

Ethics. All ZF experiments were approved by the animal-research ethics committee of Gyeongsang National University (approval GNU-190325-E0014).

Inoculum preparation for zebrafish infection. Regarding the preparation of infection stock, *Mab* CIP104536 R expressing GFP was inoculated to mid-log phase to an OD₆₀₀ of 0.8. The cell pellet was harvested by centrifugation at 4,000 \times rpm for 15 min. The 200- μ L aliquots of pellet suspension was transferred into microcentrifuge tubes prior to separating bacilli by passing the suspension through a 26-gauge needle and sonication at 40 kHz for 30 s three times (Branson CPX3800, Danbury, CT, USA). The homogenized bacteria then were added with 1 mL of 7H9^{G^T/ADC} per each tube before collecting the supernatant by centrifuging at 100 \times g for 3 min. Finally, single cells from supernatant were harvested by centrifugation at 4,000 \times rpm for 5 min. The pellet was resuspended in 200 μ L 7H9^{ADC}, and 5 μ L was aliquoted into microtubes previously stored at -80°C. The stock concentration was determined by plating 10-fold serial dilutions on 7H10-OADC with kanamycin 50 μ g/mL and counting CFU. Infection stock then was diluted with PBST (phosphate-buffered saline with 0.05% Tween 80) and resuspended in Phenol Red 0.085% to obtain 130 CFU/nL.

Microinjection of *Mab* into ZF through caudal vein infection for drug efficacy. Zebrafish embryos at 30 to 48 h postfertilization were dechorionated, anesthetized in 270 mg/liter tricaine, and then infected with 270 mg/L tricaine. Around 3 nL of *Mab* (R) CIP104536^T (approximately 400 CFU) was injected via the caudal veins

using a Tritech Research Digital microINJECTOR (MINJ-D; Tritech Research, Los Angeles, CA, USA). The equal volume was checked by injection of 3 nL inoculum in sterile PBST and plated on 7H10-OADC supplemented with 50 $\mu\text{g}/\text{mL}$ kanamycin. The infected embryos were transferred into 96-well plates (2 fish/well) and incubated at 28.5°C to treat the compound and to follow the embryos survival. ETB and DS at the final concentration of 6.25, 12.5, 25, and 50 μM were added directly into the blue fish water (using methylene blue 300 $\mu\text{L}/\text{liter}$). The compound efficacy was compared with TGC control at the concentration of 25 and 50 μM . Fish water and compound were renewed once daily, and then the drug was absorbed orally by infected embryos. The negative control is infected untreated embryos.

Drug efficacy assessment in *Mab-mWasabi*-infected ZF. The *in vivo* assessment efficacy of compounds were determined by following bacterial burden enumeration and the kinetics of embryos survival: (i) For quantification of the bacterial load, a group of 20 infected embryos (5 dpi) were collected and individually homogenized in 2% Triton X-100–PBS[†] using a handheld homogenizer (D1000; Benchmark Scientific, Sayreville, NJ, USA). Serial 10-fold dilutions of suspension were plated out on 7H10-OADC supplemented with 50 $\mu\text{g}/\text{mL}$ kanamycin and BBL *Mycobacteria* growth indicator tubes MGIT PANTA (polmyxin B, amphotericin B, nalidixic acid, trimethoprim, and azlocillin; Becton Dickinson, Franklin Lakes, NJ, USA) and then incubated for 3 to 5 days at 37°C to enumerate the CFU using one-way analysis of variance (ANOVA) comparing between treated and untreated control. (ii) Dead embryos (no heartbeat) were recorded daily for 13 days to determine the survival curve. The CFU quantification and the survival curve were plotted by Prism using the method from Kaplan and Meier and the log-rank (Mantel-Cox) test, respectively, to compare the differences between untreated control and treated embryos.

SUPPLEMENTAL MATERIAL

Supplemental material is available online only.

SUPPLEMENTAL FILE 1, PDF file, 0.5 MB.

ACKNOWLEDGMENTS

This research was supported by grant 2020R1A2C1004077 from the National Research Foundation of South Korea, grant from 2020ER520601 the Korea Disease Control and Prevention Agency (2020 to 2021), and grant HI22C0884 from the Korea Health Industry Development Institute. T.Q.N., B.T.B.H., Y.P., B.E.H., S.J., and A.C. were supported by the BK21 Four Program.

REFERENCES

- Nessar R, Cambau E, Reytrat JM, Murray A, Gicquel B. 2012. *Mycobacterium abscessus*: a new antibiotic nightmare. *J Antimicrob Chemother* 67:810–818. <https://doi.org/10.1093/jac/dkr578>.
- Quang NT, Jang J. 2021. Current molecular therapeutic agents and drug candidates for *Mycobacterium abscessus*. *Front Pharmacol* 12:724725. <https://doi.org/10.3389/fphar.2021.724725>.
- Gomez MAR, Ibba M. 2020. Aminoacyl-tRNA synthetases. *RNA* 26:910–936. <https://doi.org/10.1261/rna.071720.119>.
- Hu QH, Liu RJ, Fang ZP, Zhang J, Ding YY, Tan M, Wang M, Pan W, Zhou HC, Wang ED. 2013. Discovery of a potent benzoxaborole-based anti-pneumococcal agent targeting leucyl-tRNA synthetase. *Sci Rep* 3:2475. <https://doi.org/10.1038/srep02475>.
- Palencia A, Li X, Bu W, Choi W, Ding CZ, Easom EE, Feng L, Hernandez V, Houston P, Liu L, Meewan M, Mohan M, Rock FL, Sexton H, Zhang S, Zhou Y, Wan B, Wang Y, Franzblau SG, Woolhiser L, Gruppo V, Lenaerts AJ, O'Malley T, Parish T, Cooper CB, Waters MG, Ma Z, Ioerger TR, Sacchetti JC, Rullas J, Angulo-Barturen I, Pérez-Herrán E, Mendoza A, Barros D, Cusack S, Plattner JJ, Alley MRK. 2016. Discovery of novel oral protein synthesis inhibitors of *Mycobacterium tuberculosis* that target leucyl-tRNA synthetase. *Antimicrob Agents Chemother* 60:6271–6280. <https://doi.org/10.1128/AAC.01339-16>.
- Ganapathy US, Del Rio RG, Cacho-Izquierdo M, Ortega F, Lelièvre J, Barros-Aguirre D, Lindman M, Dartois V, Gengenbacher M, Dick T. 2021. A leucyl-tRNA synthetase inhibitor with broad-spectrum antimycobacterial activity. *Antimicrob Agents Chemother* 65:e02420-20. <https://doi.org/10.1128/AAC.02420-20>.
- Kim T, Hanh BTB, Heo B, Quang N, Park Y, Shin J, Jeon S, Park JW, Samby K, Jang J. 2021. A screening of the MMV pandemic response box reveals epetaborole as a new potent inhibitor against *Mycobacterium abscessus*. *Int J Mol Sci* 22:5936. <https://doi.org/10.3390/ijms22115936>.
- O'Dwyer K, Spivak AT, Ingraham K, Min S, Holmes DJ, Jakielaszek C, Rittenhouse S, Kwan AL, Livi GP, Sathe G, Thomas E, Van Horn S, Miller LA, Twynholm M, Tomayko J, Dalessandro M, Caltabiano M, Scangarella-Oman NE, Brown JR. 2015. Bacterial resistance to leucyl-tRNA synthetase inhibitor GSK2251052 develops during treatment of complicated urinary tract infections. *Antimicrob Agents Chemother* 59:289–298. <https://doi.org/10.1128/AAC.03774-14>.
- Day LO. 2022. AN2 Therapeutics Provides Update on Epetaborole Ex-U.S. Development Plan in Treatment-Refractory MAC Lung Disease. *GlobeNewswire*.
- Kumar M, Rao M, Purnapatre KP, Barman TK, Joshi V, Kashyap A, Chaira T, Bambal RB, Pandya M, Al Khodor S, Upadhyay DJ, Masuda N. 2019. DS86760016, a leucyl-tRNA synthetase inhibitor with activity against *Pseudomonas aeruginosa*. *Antimicrob Agents Chemother* 63:e02122-18. <https://doi.org/10.1128/AAC.02122-18>.
- Purnapatre KP, Rao M, Pandya M, Khanna A, Chaira T, Bambal R, Upadhyay DJ, Masuda N. 2018. *In vitro* and *in vivo* activities of DS86760016, a novel leucyl-tRNA synthetase inhibitor for gram-negative pathogens. *Antimicrob Agents Chemother* 62:e01987-17. <https://doi.org/10.1128/AAC.01987-17>.
- Soni A, Agarwal A, Deshmukh SS, Purnapatre KP, Marumoto S. 2018. Tricyclic benzoxaboroles as antibacterial agents. US patent application 15393966.
- Cho J, Kim K, Park J, Kim MJ. 2021. Asymmetric synthesis of biaryl diols via dynamic kinetic resolution. *Bull Korean Chem Soc* 42:1028–1032. <https://doi.org/10.1002/bkcs.12337>.
- Kim TS, Choe JH, Kim YJ, Yang CS, Kwon HJ, Jeong J, Kim G, Park DE, Jo EK, Cho YL, Jang J. 2017. Activity of LCB01-0371, a novel oxazolidinone, against *Mycobacterium abscessus*. *Antimicrob Agents Chemother* 61:e02752-16. <https://doi.org/10.1128/AAC.02752-16>.
- Catherinot E, Clarissou J, Etienne G, Ripoll F, Emile JF, Daffé M, Perronne C, Soudais C, Gaillard JL, Rottman M. 2007. Hypervirulence of a rough variant of the *Mycobacterium abscessus* type strain. *Infect Immun* 75:1055–1058. <https://doi.org/10.1128/IAI.00835-06>.
- Kim SH, Bae S, Song M. 2020. Recent development of aminoacyl-tRNA synthetase inhibitors for human diseases: a future perspective. *Biomolecules* 10:1625. <https://doi.org/10.3390/biom10121625>.
- Wu W, He S, Li A, Guo Q, Tan Z, Liu S, Wang X, Zhang Z, Li B, Chu H. 2022. A novel leucyl-tRNA synthetase inhibitor, MRX-6038, expresses anti-*Mycobacterium abscessus* activity *in vitro* and *in vivo*. *Antimicrob Agents Chemother* 66:e00601-22. <https://doi.org/10.1128/aac.00601-22>.
- Sullivan JR, Lupien A, Kalthoff E, Hamela C, Taylor L, Munro KA, Schmeing TM, Kremer L, Behr MA. 2021. Efficacy of epetaborole against *Mycobacterium abscessus* is increased with norvaline. *PLoS Pathog* 17:e1009965. <https://doi.org/10.1371/journal.ppat.1009965>.

19. Ganapathy US, Gengenbacher M, Dick T. 2021. Epetraborole is active against *Mycobacterium abscessus*. *Antimicrob Agents Chemother* 65:e01156-21. <https://doi.org/10.1128/AAC.01156-21>.
20. Bernut A, Herrmann JL, Kissa K, Dubremetz JF, Gaillard JL, Lutfalla G, Kremer L. 2014. *Mycobacterium abscessus* cording prevents phagocytosis and promotes abscess formation. *Proc Natl Acad Sci U S A* 111:E943–E952.
21. Jeong J, Kim G, Moon C, Kim HJ, Kim TH, Jang J. 2018. Pathogen box screening for hit identification against *Mycobacterium abscessus*. *PLoS One* 13:e0195595. <https://doi.org/10.1371/journal.pone.0195595>.
22. Esther CR, Esserman DA, Gilligan P, Kerr A, Noone PG. 2010. Chronic *Mycobacterium abscessus* infection and lung function decline in cystic fibrosis. *J Cyst Fibros* 9:117–123. <https://doi.org/10.1016/j.jcf.2009.12.001>.
23. Koh WJ, Jeong BH, Kim SY, Jeon K, Park KU, Jhun BW, Lee H, Park HY, Kim DH, Huh HJ, Ki CS, Lee NY, Kim HK, Choi YS, Kim J, Lee SH, Kim CK, Shin SJ, Daley CL, Kim H, Kwon OJ. 2017. Mycobacterial characteristics and treatment outcomes in *Mycobacterium abscessus* lung disease. *Clin Infect Dis* 64:309–316. <https://doi.org/10.1093/cid/ciw724>.
24. Halloum I, Carrère-Kremer S, Blaise M, Viljoen A, Bernut A, Le Moigne V, Vilchèze C, Guérardel Y, Lutfalla G, Herrmann JL, Jacobs WR, Kremer L. 2016. Deletion of a dehydratase important for intracellular growth and cording renders rough *Mycobacterium abscessus* avirulent. *Proc Natl Acad Sci U S A* 113: E4228–E4237. <https://doi.org/10.1073/pnas.1605477113>.
25. Madani A, Negatu DA, El Marrouni A, Miller RR, Boyce CW, Murgolo N, Bungard CJ, Zimmerman MD, Dartois V, Gengenbacher M, Olsen DB, Dick T. 2022. Activity of tricyclic pyrrolopyrimidine gyrase B inhibitor against *Mycobacterium abscessus*. *Antimicrob Agents Chemother* 66:e00669-22. <https://doi.org/10.1128/aac.00669-22>.
26. Dick T, Shin SJ, Koh WJ, Dartois V, Gengenbacher M. 2020. Rifabutin is active against *Mycobacterium abscessus* in mice. *Antimicrob Agents Chemother* 64:e01943-19. <https://doi.org/10.1128/AAC.01943-19>.